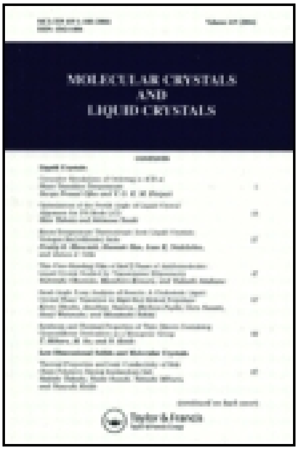

Molecular Crystals and Liquid Crystals
Publication details, including instructions for authors and subscription information:
http://www.tandfonline.com/loi/gmcl20

# Cocrystals of 2-AMINO-5-Nitropyridine with Benzenesulfonic Acids for Second Order Nonlinear Optical Materials

Hideko Koshima [a] , Hironori Miyamoto [a] , Ichizo Yagi [b] & Kohei Uosaki [b]

[a] Department of Applied Chemistry, Faculty of Engineering, Ehime University, Matsuyama, 790-8577, Japan

[b] Graduate School of Science, Division of Chemistry, Hokkaido University, N10W8, Kita-ku, Sapporo, Hokkaido, 060-0810, Japan

To cite this article: Hideko Koshima, Hironori Miyamoto, Ichizo Yagi & Kohei Uosaki (2004): Cocrystals of 2-AMINO-5-Nitropyridine with Benzenesulfonic Acids for Second Order Nonlinear Optical Materials, Molecular Crystals and Liquid Crystals, 414:1, 77-86

To link to this article: http://dx.doi.org/10.1080/15421400490427386

*Mol. Cryst. Liq. Cryst.*, Vol. 414, pp. 77–86, 2004

ISSN: 1542-1406 print/1563-5287 online
DOI: 10.1080/15421400490427386

# COCRYSTALS OF 2-AMINO-5-NITROPYRIDINE WITH BENZENESULFONIC ACIDS FOR SECOND ORDER NONLINEAR OPTICAL MATERIALS

*Hideko Koshima and Hironori Miyamoto*
*Department of Applied Chemistry, Faculty of Engineering,*
*Ehime University, Matsuyama 790-8577, Japan*

*Ichizo Yagi and Kohei Uosaki*
*Graduate School of Science, Division of Chemistry,*
*Hokkaido University, N10W8, Kita-ku, Sapporo,*
*Hokkaido 060-0810, Japan*

*Cocrystals were prepared from 2-amino-5-nitropyridine (2A5NP) and achiral benzenesulfonic acids (Ar-$SO_3H$), which were designed for second-order nonlinear optical materials. Both components are commonly crystallized in 1:1 ionic forms of $2A5NPH^+\bullet Ar–SO_3^-$. The cocrystal of 2A5NP with 2-nitrobenzenesulfonic acid belongs to acentric space group Pc, in which $2A5NPH^+$ cation and anion are alternately stacked in an almost parallel and superimposed manner to form column and layer structures. The cocrystal of 2A5NP with 3-nitrobenzenesulfonic acid is crystallized into chiral space group $P2_12_12_1$. The $2A5NPH^+$ cation and anion are also alternately stacked with some dihedral angle to form column structures. These organic–organic cocrystals are controlled by the aromatic–aromatic interactions as well as multidirectional ionic and hydrogen bondings between the $2A5NPH^+$ cations and $Ar-SO_3^-$ anions. Second-harmonic generation (SHG) powers of the crystals measured by second-harmonic generation with evanescent wave (SHEW) technique were, however, smaller than that of area. The reasons for small SHG powers are discussed based on the molecular arrangements.*

*Keywords*: aminonitropyridine-benzenesulfonic acids; crystal structures; organic–organic cocrystals; second-order nonlinear optical cocrystals; SHG powers

This work was supported by a Grant-in-Aid for Scientific Research from the Ministry of Education, Culture, Sports, Science and Technology of Japan, and the Kurata Memorial Hitachi Science and Technology Foundation.

Address correspondence to Hideko Koshima, e-mail: koshima@eng.ehime-u.ac.jp

# INTRODUCTION

Chiral and noncentrosymmetric crystals formed from achiral organic compounds are useful for second-order nonlinear optical (NLO) materials [1–5]. Our study for the preparation of chiral and noncentrosymmetric cocrystals by combining two different achiral molecules has revealed that the cocrystal approach provides higher possibilities for crystal structure design rather than single component approach [6–8]. Organic–inorganic cocrystals of 2-amino-5-nitropyridine (2A5NP) **1** with inorganic acids such as phosphoric acid have been published for NLO materials by Masse and coworkers [9]. Recently we have prepared several organic–organic cocrystals of **1** with achiral benzenesulfonic acids and found to be quite large second-harmonic generation (SHG) power of the cocrystal with *p*-phenolsulfonic acid [10]. The organic–organic cocrystal approach by using 2A5NP and benzenesulfonic acids confirmed the validity for design of second-order NLO materials. Herein, we report new cocrystals of **1** with other achiral benzenesulfonic acids **a**–**d** (Ar-$SO_3H$) (Scheme 1).

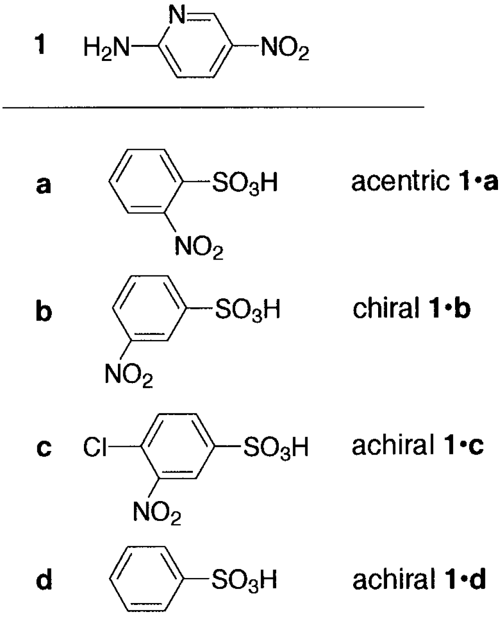

**SCHEME 1**

# EXPERIMENTAL

## Preparation of Cocrystals

An equimolar mixture of 2-amino-5-nitropyridine **1** (2 mmol) and *o*-nitrobenzenesulfonic acid **a** (2 mmol) was dissolved in a mixed solvent (20 ml) of methanol and 2M HCL (20:1) with gentle heating followed by evaporation to give cocrystal **1a**. The other three cocrystals **1b**–**1d** were also prepared by the same procedure. Several mm sizes of single crystals were also obtained by slow evaporation at room temperature. The crystals were characterized by the measurements of melting point (mp) and IR and X-ray crystallographic analysis.

**1a:** light yellow plate crystals; mp 206–207°C; IR (KBr) 1025, 1143, 3225, 3294 $\mathrm{cm}^{-1}$.
**1b:** colorless plate crystals; mp 172–173°C; IR (KBr) 1037, 1129, 3129, 3328 $\mathrm{cm}^{-1}$.
**1c:** colorless plate crystals; mp 155–156°C; IR (KBr) 1042, 1130, 3127, 3330 $\mathrm{cm}^{-1}$.
**1d:** colorless plate crystals; mp 192–198°C; IR (KBr) 1347, 1525, 3084, 3265 $\mathrm{cm}^{-1}$.

## X-Ray Crystallographic Analysis

X-ray data of the crystals **1a–1d** were collected on a Rigaku RAXIS RAPID imaging plate with Cu K$\alpha$ radiation to a maximum $2\theta$ of 136.5°. A total of $30 \times 5.00^\circ$ oscillation images were collected, each being exposed for 15 min. The reflection data were corrected for Lorentz polarization effects and secondary extinction. The structure was solved by direct methods and expanded using Fourier techniques. The nonhydrogen atoms were refined anisotropically, and hydrogen atoms were not refined. The final cycle of full-matrix least-squares refinement was based on all reflections ($2\theta < 136.5^\circ$) and variable parameters, and it converged with unweighted and weighted agreement factors of: $R = \Sigma||F_o| - |F_c||/\Sigma|F_o|$ for $I > 2.0\sigma(I)$ and $R_w = \{\Sigma w(F_o^2 - F_c^2)^2/\ \Sigma w(F_o^2)^2\}^{1/2}$. All calculations were performed by using teXsan crystallographic software. The crystal data were deposited at the Cambridge Crystallographic Data Centre. The deposition numbers are CCDC 218552–218555 for **1a**–**1d**, respectively.

## SHG Property

SHG powers of the crystals **1a** and **1b** were measured in powder form by total reflection method using a hemicylindrical prism (BK7 glass), based on second-harmonic generation with evanescent wave (SHEW) technique

[11]. The fundamental wave ($\lambda = 1200\,\text{nm}$) was used with the fixed incident angle of 60°. The dependence of laser powers on the signals at 600 nm were measured and compared with well-known urea [12], *m*-nitroaniline (*m*NA) [13], and 4-(N,N-dimethylamino)-3-acetamidonitrobenzene (DAN) [14] as standard SHG crystals.

## RESULTS AND DISCUSSION

The key molecule is 2-amino-5-nitropyridine **1**, which has a nitro group as an electron donor and an amino group as an electron acceptor to induce NLO character. Furthermore, the pyridine nitrogen acts as a cationic binding site, the nitro group as a hydrogen acceptor, and the amino group as a hydrogen donor. The achiral benzenesulfonic acids **a**–**d** were selected as strong anionic connectors.

X-Ray crystallographic analysis of the crystals **1a** and **1b** confirmed the noncentrosymmetric and chiral nature due to belonging to space groups of $Pc$ and $P2_12_12_1$, respectively. In contrast, other two crystals **1c** and **1d** were achiral due to each space group of $P2_1/n$, which means that they are inherently NLO inactive. The details of crystal data are summarized in Table 1. In all four crystals, both components are crystallized in 1:1 ratio of $2A3NPH^+$ cation and $Ar\text{-}SO_3^-$ anion. The ionic species are formed by the transformation of the proton of sulfonate acid group of **a**–**d** to the nitrogen atom of pyridine of **1**. The ionic character induces the fairly high melting points. Three kinds of intermolecular bondings are commonly formed between the cation and anion in all four crystals. One is the pyridinium salt bridge ($PyN^+{-}H\cdots{}^-O_a{-}S$) between the pyridium cation and the sulfonate anion. Other two are the hydrogen bonds ($N{-}H_a\cdots{}^-O_b{-}S$ and $N{-}H_b\cdots{}^-O_c{-}S$) between the $NH_2$ group of $2A5NPH^+$ cation and the $Ar{-}SO_3^-$ anion. The distances of salt bridges and hydrogen bonds are in the range of 1.8 to 1.9 Å and 1.9 to 2.1 Å, respectively (Table 2).

Figure 1 shows the molecular arrangement in the noncentrosymmetric crystal **1a**. The cationic and anionic species of **1** and **a** are alternately stacked to form two independent columns A and B in the asymmetric unit (Figures 1(a) and 1(b)). The pyridine ring of **1** and the benzene ring of **a** in the A and B columns are almost completely superimposed and arranged in a nearly parallel manner with the dihedral angels of 4.5(6)° and 4.3(6)°, respectively. In each column of A and B, separate layers of $2A5NPH^+$ cations and sulfonate anions are formed along the *a* axis (Figures 1(c) and 1(d)). Further, the pyridine rings between A and B columns crossed each other with the dihedral angle of 50.0(6)°, and the benzene rings also with 41.9(6)°. Pyridinium salt bridge ($PyN^+{-}H\cdots{}^-O_a{-}S$) and hydrogen bond ($N{-}H_a\cdots{}^-O_b{-}S$) are formed between the neighboring A and B

**TABLE 1** Crystal Data of the Cocrystals

| | **1a** | **1b** | **1c** | **1d** |
|---|---|---|---|---|
| Formula | $C_{11}H_{10}O_7N_4S$ | $C_{11}H_{10}O_7N_4S$ | $C_{11}H_9O_7N_4SCl$ | $C_{11}H_{11}O_5N_3S$ |
| $M$ | 342.28 | 342.28 | 376.3 | 297.29 |
| Crystal color | light yellow | colorless | colorless | colorless |
| Crystal habit | platelet | platelet | platelet | platelet |
| Crystal size/mm | 0.5 × 0.1 × 0.3 | 0.7 × 0.6 × 0.1 | 0.5 × 0.3 × 0.1 | 0.5 × 0.2 × 0.1 |
| Crystal syst. | monoclinic | orthorhombic | monoclinic | monoclinic |
| Space group | $P_c$ (#7) | $P2_12_12_1$ (#19) | $P2_1$/n (#14) | $P2_1$/n (#14) |
| $a$/Å | 7.0476(8) | 7.9442(8) | 14.4536(8) | 6.8079(8) |
| $b$/Å | 12.745(4) | 27.130(3) | 8.9367(4) | 7.2019(6) |
| $c$/Å | 15.092(3) | 6.7390(8) | 23.903(3) | 26.801(4) |
| $\beta$/deg | 89.172(5) | 90.0 | 100.408(5) | 92.684(4) |
| Cell vol/$Å^3$ | 1355.5(5) | 1452.4(3) | 3036.3(3) | 1312.6(3) |
| Calcd. density/g $cm^{-3}$ | 1.677 | 1.565 | 1.648 | 1.504 |
| $Z$ | 4 | 4 | 8 | 4 |
| Data/params. | 4599/416 | 2167/210 | 5295/434 | 2280/191 |
| $R$ | 0.067 | 0.054 | 0.061 | 0.038 |
| $R_w$ | 0.187 | 0.226 | 0.165 | 0.048 |

columns (Figures 1(a) and 1(b)), and another hydrogen bond ($N-H_b\cdots{}^-O_c-S$) between the neighboring B columns (Figures 1(c) and 1(d)). The conformations of $2A5NPH^+$ species in A and B columns are almost flat because the dihedral angles of the pyridine ring and nitro group are only 5.0(6)° and 3.7(4)°, and those of pyridine ring and amino group are 12.1(4)° and 4.9(4)°, respectively. On the other hand, the phenyl rings and the nitro groups of sulfonic anions are nearly perpendicular with the dihedral angles of 78.5(4)° and 78.4(4)°, respectively. These shapes of

**TABLE 2** Intermolecular Distances and Angles ($D-H\cdots O$) of the Salt Bridges and Hydrogen Bondings in the Cocrystals

| | **1a** | | **1b** | | **1c** | | **1d** | |
|---|---|---|---|---|---|---|---|---|
| Interactions | Å | deg | Å | deg | Å | deg | Å | deg |
| $PyN^+-H\cdots{}^-O_a-S$ | 1.90 (2.83) | 170 | 1.83 (2.72) | 164 | 1.81 (2.90) | 171 | 1.83 (2.72) | 169 |
| $N-H_a\cdots{}^-O_b-S$ | 1.96 (2.86) | 170 | 1.92 (2.84) | 170 | 1.92 (2.86) | 165 | 1.99 (2.81) | 166 |
| $N-H_b\cdots{}^-O_c-S$ | 1.95 (2.81) | 151 | 2.07 (2.88) | 165 | 1.95 (2.84) | 168 | 2.00 (2.87) | 175 |
| $PyN^+-H\cdots{}^-O_a-S$ | 1.89 (2.83) | 169 | | | 1.89 (2.95) | 170 | | |
| $N-H_a\cdots{}^-O_b-S$ | 1.92 (2.81) | 154 | | | 2.05 (2.98) | 173 | | |
| $N-H_b\cdots{}^-O_c-S$ | 1.96 (2.87) | 167 | | | 1.93 (2.82) | 172 | | |

The value in the parenthesis present the distance between the N and O atom.

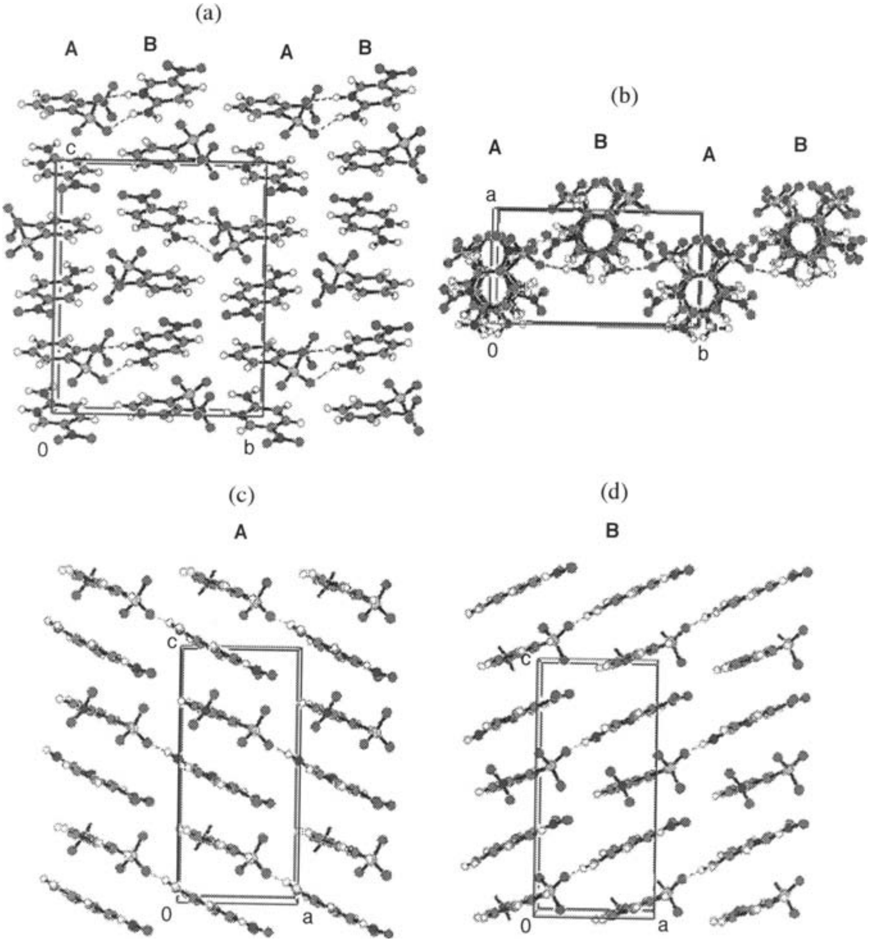

**FIGURE 1** Molecular arrangements along (a) the *a* axis and (b) the *c* axis and on the *bc* plane of (c) A pairs and (d) B pairs in **1a**.

cationic and anionic species reflect the parallel stacking arrangement in the crystal.

Figure 2 shows the molecular arrangement in the chiral crystal **1b**. The 2A5NPH$^+$ cation and the sulfonate anion are alternately stacked to form four columns along the *a* axis. The pyridine ring of **1** and the benzene ring of **b** are nearly superimposed with some dihedral angle (148.4(1)°) due to the large $SO_3^-$ anion. A cation is connected to a neighboring anion in the same unit cell through the pyridinium salt bridge ($PyN^+{-}H\bullet\bullet\bullet{}^-O_a{-}S$) and the hydrogen bond ($N{-}H_a\bullet\bullet\bullet{}^-O_b{-}S$), and the cation is also connected to

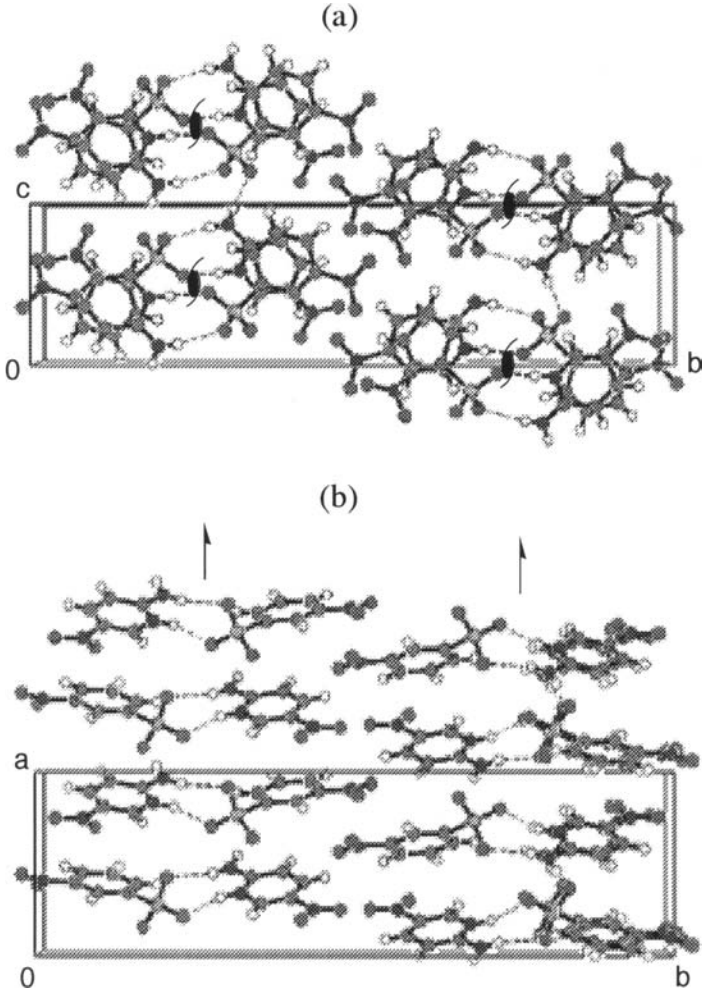

**FIGURE 2** Molecular arrangements on (a) the *bc* plane and (b) *ab* plane in **1b**.

another anion in the next unit cell through the hydrogen bond ($N{-}H_b{\cdots}{}^-O_c{-}S$) (Figure 2(a)), forming binding zones along the *a* and *c* axis. At the opposite side of the binding zones, the nitro groups of cation and anion that are not participating in any hydrogen bondings aggregate in mutual repulsion and abstraction to form nitro group zones along the *a* and *c* axis. The intermolecular N---O, N---N, and O---O distanes are 2.97–3.52, 3.49, and 2.89–3.34 Å, respectively. The pyridine plane and the nitro group of the $2A5NPH^+$ cation, and the phenyl plane and the nitro group of anion are in some torsional conformations with the dihedral angles of 138.34(6)° and 8.8(1)°, respectively.

It is interesting that the small structural difference between *o*- and *m*-substituted position of nitro group in the **a** and **b** molecules leads to the different molecular arrangements between **1a** and **1b**. Achiral cocrystals **1c** and **1d** have also alternate stacking structures of 2A5NPH$^+$ cations and benzenesulfonate anions. However, the ionic species are arranged centrosymmetrically in the lattice. Namely, in the case of organic–organic cocrystals **1a**–**1d**, the $\pi$–$\pi$ interaction between the pyridine and phenyl moieties, as well as the multidimensional ionic and hydrogen bonds, control the crystal structures to lead to the alternate stacking of 2A5NPH$^+$ cations and Ar$-$SO$_3$$^-$ anions and the formation of column and layer structures. On the other hand, in the organic–inorganic crystals, the inorganic anions such as nitrate, dichromate, and phosphate lacking of aromatic moieties play the role of controlling the crystal structures by the multidimensional hydrogen bonds [9].

Finally, SHG powers of the crystals **1a** and **1b** were measured in powder form by SHEW technique [11]. Fixed incident angle of 60° was used, and total reflection at 600 nm was measured. Because the refraction indices of **1a** and **1b** are probably similar due to the analogous component molecules, angle dependence of the SHG strength was not measured and parameter fitting was not applied. Relative SHG values to well-known urea [12], *m*NA [12], and DAN [13] are shown in Table 3. The SHG powers of **1a** and **1b** are smaller than that of urea. Absorption spectra of powdered crystals of **1a** and **1b** were measured by reflection method using barium sulfate as a reference. The cutoff wavelengths determined from the absorption edges were around 435 and 414 nm, favorable to NLO materials.

The small SHG powers of **1a** and **1b** should reflect the packing arrangements of 2A5NPH$^+$ cation as a SHG chromophore. As we previously reported [10], in the large SHG cocrystal of **1** with *p*-phenolsulfonic acid, herringbone structure of 2A5NPH$^+$ moieties was formed to induce the charge transfer enhancement. Hence, it is important for the generation of large SHG powers to be arranged into independent columnar structure

**TABLE 3** SHG Powers of the Cocrystals

| | Relative SHG power to | | | |
|---|---|---|---|---|
| Cocrystal | Urea | *m*-nitroaniline | DAN | Cutoff wavelength (nm) |
| **1a** | 0.76 | 0.20 | 0.08 | 435 |
| **1b** | 0.38 | 0.10 | 0.04 | 414 |

such as herringbone network of 2A5NPH$^+$ moieties. However, in the case of crystal **1a**, the pyridine and phenyl moieties of **1** and **a** are almost completely superimposed along the *c* axis to hinder the interaction among the 2A5NPH$^+$ moieties (Figures 1(a) and 1(b)). In the crystal **1b**, the alternate and nearly superimposed stackings of 2A5NPH$^+$ cations and sulfonate anions also may disturb the charge transfer enhancement of 2A5NPH$^+$ moieties to result in the low SHG power (Figure 2). Furthemore, the electron-withdrawing nitro group of **a** and **b** may lead to decrease the SHG character. In this series of cocrystals, alternated stacking structure of 2A5NPH$^+$ cation and sulfonate anion is commonly formed because of the $\pi$–$\pi$ interaction of pyridine and phenyl moieties. In the preparation of cocrystals, combination with benzenesulfonic acid derivatives having larger substituted groups may actualize small superimposition of pyridine and phenyl moieties due to the steric hindrance, to lead to the formation of independent columnar structure of 2A5NPH$^+$ cation and sulfonate anion.

## REFERENCES

[1] Jacques, J., Collet, A., & Wilen, S. H. (1981). *Enantiomers, Racemates and Resolutions*; (New York: Wiley) pp. 14–23.

[2] (a) Koshima, H. & Matsuura, T. (1998). *J. Synth. Org. Chem.*, *56*, 268–268 (in Japanese). (b) Koshima, H. & Matsuura, T. (1998). *J. Synth. Org. Chem.*, *56*, 466–477 (in Japanese).

[3] Nicoud, J. F. & Twieg, R. J. (1985). *Quantum Electronics Principles and Applications Series*, Chemla, D. S., & Zyss, J. (Eds.), (Orlando: Academic Press).

[4] Miyata, S. (1991). *Organic Molecules for Nonlinear Optics and Photonics*, Messier, J., Kajzar, F., & Prasad, P. (Eds.), (Dordrecht: Kluwar).

[5] (a) Koshima, H., Wang, Y., Matsuura, T., Mibuka, N., & Imahashi, S. (1996). *Mol. Cryst. Liq. Cryst.*, *275,* 233–239.
(b) Koshima, H., Wang, Y., & Matsuura, T. (1996). *Mol. Cryst. Liq. Cryst.*, *277*, 63–71.

[6] (a) Koshima, H., Ding, K., Chisaka, Y., & Matsuura, T. (1996). *J. Am. Chem. Soc.*, *118*, 12059–12065.
(b) Koshima, H., Nakagawa, T., Matsuura, T., Miyamoto, H., & Toda, F. (1997). *J. Org. Chem.*, *62*, 6322–6325.

[7] (a) Koshima, H., Hayashi, E., Matsuura, T., Tanaka, K., Toda, F., Kato, M., & Kiguchi, M. (1997). *Tetrahedron Lett.*, *38*, 5009–5012.
(b) Koshima, H., Hayashi, E., & Matsuura, T. (1999). *Supramol. Chem.*, *11*, 57–66.

[8] (a) Koshima, H., Khan, S. I., & Garcia-Garibay, M. A. (1998). *Tetahedron Asymmetry*, *9*, 1851–1854.
(b) Koshima, H. & Honke, S. (1999). *J. Org. Chem.*, *64*, 790–793.
(c) Koshima, H., Honke, S., & Fujita, J. (1999). *J. Org. Chem.*, *64*, 3916.
(d) Koshima, H., Honke S., & Miyauchi, M. (2000). *Enantiomer*, *5*, 125–128.
(e) Koshima, H., Miyauchi, M., & Shiro, M. (2001). *Supramol. Chem.*, *13*, 137–142.
(f) Koshima, H. & Miyauchi, M. (2001). *Cryst. Growth & Des.*, *1*, 355.

[9] (a) Masse, R., Bagieu-Beucher, M., Pecaut, J., Levy, J. P., & Zyss, J. (1993). *Nonlin. Opt.*, *5*, 413–423.

(b) Bagieu-Beucher, M., Masse, R., & Tranqui, D. (1991). *Z. anorg. U allg. Chem.*, *606*, 59–71.

(c) Pecaut, J. & Masse, R. (1993). *Acta Cryst., B49*, 277–282.

(d) Masse, R. & Zyss, J. (1991). *Mol. Eng.*, *1*, 141–152.

(e) Kotler, Z., Hierle, R., Josse, D., & Masse, R. (1992). *J. Opt. Soc. Am., B9*, 534–547.

(f) Zyss, J., Masse, M., Bagieu-Beucher, M., & Levy, J. P. (1993). *Adv. Mat.*, *5*, 120–124.

[10] Koshima, H., Hamada, M., Yagi, I., & Uosaki, K. (2001). *Cryst. Growth Des.*, *1*, 467–471.

[11] (a) Kiguchi, M., Kato, M., & Taniguchi, Y. (1993). *Appl. Phys. Lett.*, *63*, 2165–2167.

(b) Kiguchi, M., Kato, M., Kumegawa, N., & Taniguchi, Y. (1994). *J. Appl. Phys.*, *75*, 4332–4339.

(c) Kato, M., Kiguchi, M., Sugita, N., & Taniguchi, Y. (1997). *J. Phys. Chem. B*, *101*, 8856–8859.

[12] Halbout, J. M., Blit, S., Donaldson, W., & Tang, C. L. (1979). *IEEE J. Quantum Electron.*, *QE-15*, 1176–1180.

[13] Southgate, P. D. & Hall, D. S. (1971). *Appl. Phys. Lett.*, *18*, 456–458.

[14] Baumert, J.-C., Twieg, R. J., Bjorklund, G. C., Logan, J. A., & Dirk, C. W. (1987). *Appl. Phys. Lett.*, *51*, 1484–1486.